University of New Hampshire
University of New Hampshire Scholars' Repository

Center for Coastal and Ocean Mapping | Center for Coastal and Ocean Mapping

2012

Acoustic sensing of gas seeps in the deep ocean with split-beam echosounders

Thomas C. Weber
University of New Hampshire, Durham, thomas.weber@unh.edu

Kevin W. Jerram
University of New Hampshire, Durham, kevin.jerram@unh.edu

Larry A. Mayer
University of New Hampshire, larry.mayer@unh.edu

Follow this and additional works at: https://scholars.unh.edu/ccom

 Part of the Oceanography and Atmospheric Sciences and Meteorology Commons

Recommended Citation

T. C. Weber, K. Jerram, and L. Mayer, 'Acoustic sensing of gas Seeps in the deep ocean with split-beam Echosounders', Proceedings of Meetings on Acoustics (POMA), Vol.17, Issue 1.

This Conference Proceeding is brought to you for free and open access by the Center for Coastal and Ocean Mapping at University of New Hampshire Scholars' Repository. It has been accepted for inclusion in Center for Coastal and Ocean Mapping by an authorized administrator of University of New Hampshire Scholars' Repository. For more information, please contact Scholarly.Communication@unh.edu.

Proceedings of Meetings on Acoustics

Volume 17, 2012 http://acousticalsociety.org/

ECUA 2012 11th European Conference on Underwater Acoustics
Edinburgh, Scotland
2 - 6 July 2012
Session UW: Underwater Acoustics

UW225. Acoustic Sensing of Gas Seeps in the Deep Ocean with Split-beam Echosounders

Thomas C. Weber*, Kevin Jerram and Larry Mayer

***Corresponding author's address: Center for Coastal and Ocean Mapping, University of New Hampshire, Durham, NH 03824, weber@ccom.unh.edu**

When in the form of free gas in the water column, methane seeps emanating from the seabed are strong acoustic targets that are often detectable from surface vessels using echo sounders. In addition to detecting that a seep is present at some location, it is also desirable to characterize the nature of the seep in terms of its morphology and flux rates. Here, we examine how much we can learn about seeps in the deep (> 1000 m) northern Gulf of Mexico using narrow-band split-beam echo sounders operating at fixed frequencies (18 kHz and 38 kHz). Methane seeps in this region are deeper than the methane hydrate stability zone, implying that bubbles of free gas form hydrate rinds that allow them to rise further in the water column than they otherwise would. While this behavior may aid in the classification of gas types in the seep, it is possible that the presence of hydrate rinds may also change the acoustic response of the bubbles and thereby make flux rate estimates more challenging. These and other aspects of seep characterization will be discussed.

Published by the Acoustical Society of America through the American Institute of Physics

©2012 Acoustical Society of America [DOI: 10.1121/1.4772948]
Received 16 Nov 2012; published 6 Dec 2012
Proceedings of Meetings on Acoustics, Vol. 17, 070057 (2012)

Redistribution subject to ASA license or copyright; see http://acousticalsociety.org/content/terms. Download to IP: 132.177.229.80 On: Tue, 17 Nov 2015 15:33:38

1 INTRODUCTION

During the summer of 2010, several NOAA vessels including the *Gordon Gunter*, the *Thomas Jefferson*, the *Pisces,* and the *Henry Bigelow* surveyed the water column searching for evidence of submerged oil [1] using single and split-beam echosounders. During this time, frequent observations were made of natural methane seeps that were generally known to be present in the northern Gulf of Mexico [e.g., 2]. Most, although not all, of the methane seeps observed in 2010 were located on the edges of salt domes; this suggests that the methane is sourced from the same deep reservoirs that are being actively pursued by the oil and gas industry, and makes its way to the seabed through faults associated with the movement of salt.

Submarine methane seeps play a role in the global atmospheric methane budget [3], can act as an energy source for chemosynthetic communities in the deep ocean [4], and are important to understand when assessing the anthropogenic impacts of deepwater oil and gas extraction. In the deep ocean, bubbles of methane gas originating at the seafloor may never reach the atmosphere due to dissolution and subsequent oxidation, although there may be some mechanisms by which gas transfer out of the bubble is inhibited including the presence of oil coatings on bubbles [5] and hydrate skins on the outer wall of the bubbles [6]. Due at least in part to the technical difficulties associated with their direct observation, methane seeps in the deep ocean are poorly understood in terms of their evolution as they rise through the water column, their natural variability, and the overall flux of gas from deep reservoirs into either the ocean and/or atmosphere.

In this paper, we examine what can be learned about natural seeps using split-beam echosounders, focusing on observations of two seeps made in late May 2010 onboard the *Gordon Gunter* using calibrated 18 kHz and 38 kHz Simrad EK60 split-beam echosounders. The use of echo sounders for imaging gas seeps is not new [e.g., 5, 7, 8, 9, 10, 11], but the full potential of split-beam echosounders for imaging methane seeps has generally not yet been fully exploited.

2 EXAMPLE GAS SEEPS

Two examples of methane bubble seeps observed from the *Gordon Gunter* in May 2010 are shown as echograms in figure 1 (left). These seeps were observed on the northwestern edge of the Biloxi Dome, a salt diapir in the northern Gulf of Mexico. The horizontal layers present in the echogram are caused by scattering from the marine organisms making up the deep scattering layer, with the strongest scattering appearing at depths less than 400 m, a deeper layer at approximately 800 m, and generally little or no observable scattering below 1000 m. Two seeps are readily apparent in Figure 1, labeled ‘seep 1’ and ‘seep 2’, appearing as vertical plumes that rise from the seafloor to approximately 500 m water depth; a weaker vertical plume as well as what appears to be a more discrete discharge from the seafloor are also present in the echogram.

Redistribution subject to ASA license or copyright; see http://acousticalsociety.org/content/terms. Download to IP: 132.177.229.80 On: Tue, 17 Nov 2015 15:33:38

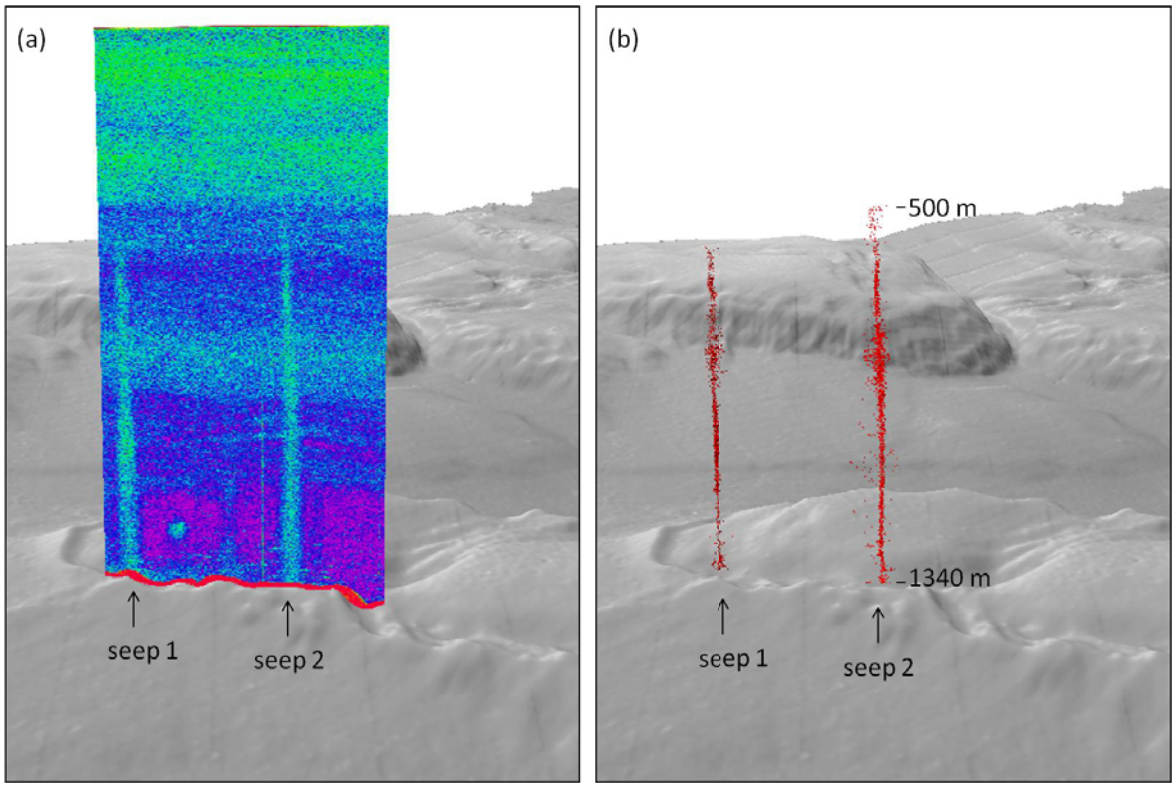

Figure 1. Bubble seeps rising from the northwestern edge of the Biloxi Dome at a depth of 1340 m in the northern Gulf of Mexico, imaged using an 18 kHz EK60 on the NOAA vessel *Gordon Gunter*. (a) Raw echograms, with color representing volume scattering strength. (b) Seep target positions resulting from split-beam positioning. Both images are shown with 6x vertical exaggeration.

The raw split-beam echosounder data corresponding to the two stronger vertical plumes are shown in Figure 2. These data include the apparent target strength (i.e., uncorrected for the target position within the beam) at both 18 kHz and 38 kHz, for which the -3 dB beamwidths are nominally 11° and 7°, respectively. Both echo sounders utilize split-aperture processing [12] to estimate the target angle in both the alongship and athwartship directions within the beam (2nd and 3rd rows of figure 2). Thus, as both seeps are approached and then passed by the vessel, the alongship target angle gradually changes from +10° to -10° for the 18 kHz echo sounder, and from +5° to -5° for the 38 kHz echosounder (note that the split-aperture processing used by the EK60 utilizes two apertures whose length is approximately half of the diameter of the entire aperture, making it possible to measure target angles well beyond the nominal 3 dB beamwidth of the transducer). The small athwartships target angle suggests its base was almost directly below the vessel track, whereas seep 2 appears to have been traversed so that the base of the seep was located along a projection 2-3° from nadir to onse side of the vessel track. In both cases, the coherency in the target angle data are suggestive of an aggregate target whose angular width is small compared to the beamwidth, in contrast with targets in the deep scattering layer which show a more random distribution of target angles. The gas seeps, then, are likely extended in depth but constrained laterally, such that the target strength normalized by the pulse length should be used for comparisons of seep strength rather than the volume scattering strength, *Sv,* which presumes that the targets are distributed laterally throughout the beam. In the data presented here, the pulse lengths at 18 kHz and 38 kHz are both 4 ms, so the target strength itself is sufficient for a relative comparison.

Redistribution subject to ASA license or copyright; see http://acousticalsociety.org/content/terms. Download to IP: 132.177.229.80 On: Tue, 17 Nov 2015 15:33:38

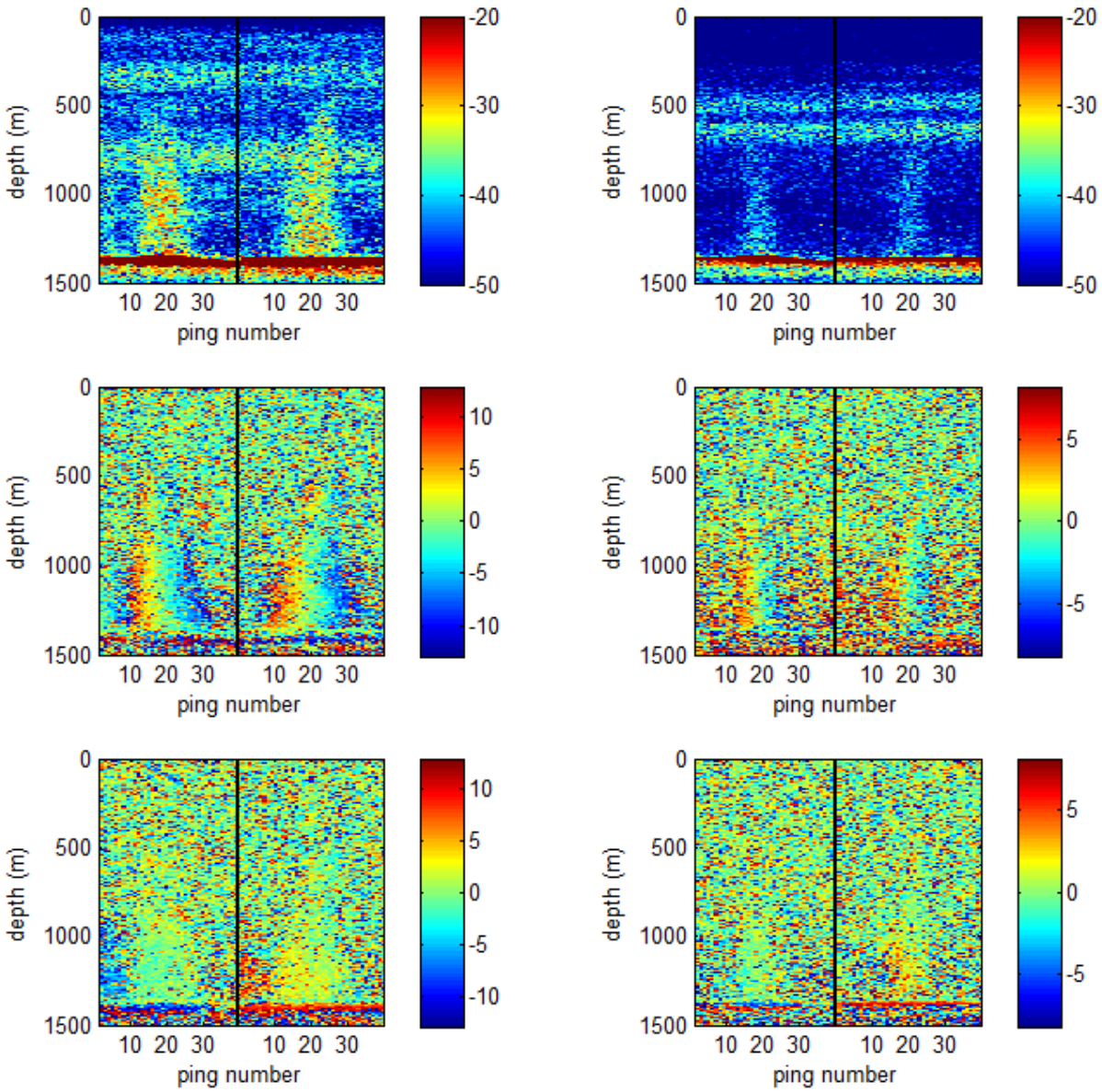

Figure 2. Raw EK60 observations at 18 kHz (left column) and 38 kHz (right column) corresponding to the two strongest seeps in Figure 1. Top row: Apparent target strength, *Sp*, in dB (uncorrected for beam pattern) of the seeps. Middle: alongship target angle in degrees. Bottom: athwartship target angle in degrees.

For the 18 kHz echosounder with 11° beamwidth, the -3 dB footprint in 1340 m of water is approximately 250 m, causing the seep to appear quite broad in the echogram shown in Figure 1. Using the known position of the vessel and the target angle data, however, the acoustic return representing the seep can be georeferenced, as shown in Figure 1(b). To do so, a threshold of *Sp* (apparent target strength, uncorrected for the beam pattern) equal to -30 dB is used to select only those targets with high signal-to-noise ratio. After georeferencing the thresholded targets, the 'scatter' of target positions for the data shown here have standard deviations of 10-40 m for much of the seep, increasing to more than 50 m when the targets coincide with targets in the deep scattering layer. The

Redistribution subject to ASA license or copyright; see http://acousticalsociety.org/content/terms. Download to IP: 132.177.229.80 On: Tue, 17 Nov 2015 15:33:38

scatter in the seep target positioning is likely due to noise limitations associated with the split-aperture processing rather than the actual spread of the bubbles within the seep. Assuming, for simplicity, isotropic point receivers, the standard deviation in target angle direction is given in radians by [12, 13]

$$\sigma_\theta = \frac{\lambda}{\pi\sqrt{d}L}$$

where L/λ is the aperture separation in wavelengths and d is the signal to noise ratio. For the 18 kHz echosounder, we assume that L/λ is approximately 2.6 (corresponding to the approximate radius of the transducer). At a depth of 1340 m (the base of the seep) and for targets on the beam maximum response axis, an SNR of ~12 dB would equate to a 40 m standard deviation in lateral positioning uncertainty and an SNR of ~25 dB would equate to a 10 m standard deviation, which is roughly the range of SNRs indicated in the 18 kHz target strength data shown in Figure 2. Thus, the 10-40 m width of the plume represents an upper bound on the lateral extent of the plume.

3 SEEP HEIGHT AND TRAJECTORY

Both seeps shown in Figure 1 and 2 appear to rise nearly 800 m, from the seabed to a depth of approximately 550 m. Recent ROV observations of nearby bubble seeps on the Biloxi Dome suggest that the bubbles are 1-10 mm in diameter upon formation at the seabed; at a terminal velocity of 20-25 cm/s this would require an approximate 1 hour transit time from the seabed to 550 m. Bubble dissolution models [e.g., 14] have shown that methane in the bubbles would become completely dissolved into the water column within minutes, unless the dissolution is slowed by hydrate forming at the methane-water boundary. Given nominal salinity and temperature profiles for the northern Gulf of Mexico, the parameterization of Tishchenko et al [15], and the assumption that the bubbles are pure methane, the hydrate dissociation depth is approximately 610 m (~7.1 degC, 35 PSU). The observations of bubble survival during ascent to 550 m suggest that the methane bubbles do form hydrate at the gas-water boundary, slowing the dissolution rate sufficiently to allow the bubble to reach much shallower depths than a hydrate-free bubble. After passing the hydrate dissolution depth and losing their hydrate shells, the methane bubbles likely require only a few minutes [e.g., 14] to completely outgas into the surrounding seawater, which is presumed to be undersaturated in methane. At a terminal velocity of 20-25 cm/s, this rapid dissolution implies that the bubbles traverse approximately 50-100 m above the hydrate dissociation depth, reaching water depths of 550-500 m; this is in accordance with the behavior we observe acoustically. The bubble size is expected to become smaller as it rises at these shallower depths [14], as the reduction in size due to gas transfer overcomes the increase in size due to the reduction in hydrostatic pressure, causing an increase in the resonance frequency of the bubble. Thus, the terminal height of the bubble plume may not be observable at either 18 kHz or 38 kHz because of the significant increases of resonance frequencies for bubbles with radii approaching zero.

As gas bubbles rise due to their buoyancy, they are presumed to act as Lagrangian drifters in the local ocean currents, making them natural current meters. The three-dimensional trajectories of the bubbles for both seep 1 and seep 2 have been estimated by bin-averaging the georeferenced target data into 10 m depth bins, and computing the seep's relative position in eastings and northings as a function of depth (Figure 3). The trajectories show that the bubbles move monotonically westward by ~60 m as they rise approximately 800 m from the seabed, with qualitatively good agreement between seep 1 and seep 2. The bubbles also move 10-20 m to the south in the lower 400 m, and then move 20-30 m back to the north in the upper 400 m of their trajectory, with seep 2 experiencing greater N-S excursions than seep 1. Assuming that the bubbles are rising at a terminal velocity of approximately 20 cm/s, requiring 4000 seconds to traverse the 800 m vertical trajectory, the westward component of the ocean current between 540-1340 m in both seep locations must have been approximately 1.5 cm/s.

Redistribution subject to ASA license or copyright; see http://acousticalsociety.org/content/terms. Download to IP: 132.177.229.80 On: Tue, 17 Nov 2015 15:33:38

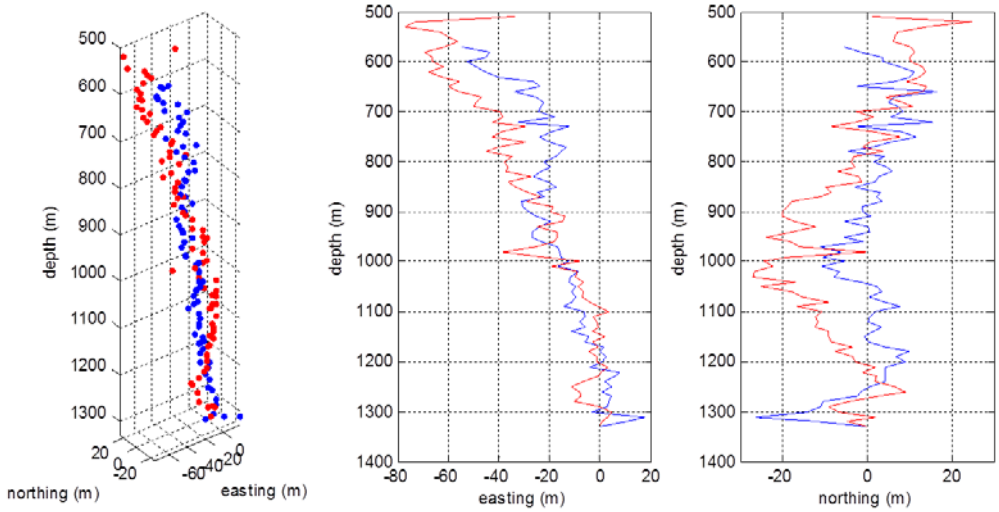

Figure 3. Seep trajectories for seep 1 (blue) and seep 2 (red).

4 FREQUENCY RESPONSE

The raw EK60 observations shown in Figure 2 suggest that the acoustic scattering strengths of the seeps are stronger at 18 kHz than at 38 kHz. To more accurately examine this, the apparent target strengths must be corrected for beam pattern effects, which cause the bubbles to appear as weaker scatterers when they are away from the maximum response axis of the transducer. To provide an estimate of the true target strength, data collected during a standard target sphere calibration [16] is used to fit a piston-transducer beam model to the nominally circular echosounders, resulting in an estimate of ka = 16.5 for the 18 kHz transducer and ka = 25.3 for the 38 kHz transducer, where k is the acoustic wave number and a is the transducer radius. The athwartship and alongship target angles are then used to correct for the apparent target amplitude reduction caused by the beam pattern, providing estimates of the seep target strength at 18 and 38 kHz without the beam pattern bias.

The target strength difference between 18 and 38 kHz for both seeps shown in Figure 1 is shown in Figure 4, for only those data whose uncorrected target strength (as shown in Figure 2) at 38 kHz was greater than -30 dB. Because the scattering response of the bubbles at 38 kHz becomes masked by the scattering from organisms in the deep scattering layer, only target strength differences at depths below 720 m are shown. While there is some small (few dB) variation in the target strength difference as a function of depth, the target strength at 18 kHz is, on average 6-10 dB higher than at 38 kHz.

Considering the frequency-dependent target strengths of methane bubbles with radii of 0.1, 1, 3, and 10 mm as shown in Figure 5, the observed target strength difference are suggestive of bubbles with a radius between 1-3 mm at the seabed. If the bubbles were of constant size as they rose through the water column, the target strength difference would be expected to change. For example, a single bubble with 2.5 mm radius would have a target strength that was ~7 dB higher at 18 kHz than at 38 kHz at a depth of 1340 m, but at 800 m the same size bubble at 800 m would have a target strength difference of only ~3 dB. One plausible explanation for the relatively constant target strength difference is that the bubbles are slowly reducing in size as they rise, causing the resonance frequencies to shift upward in such a way as to counteract the reduction in resonance frequency associated with the decrease in depth. For this to occur, the gas transfer rate must be fast enough to overcome the increase in bubble size associated with Boyle's law, despite the apparent inhibited gas transfer associated with the hydrate coating.

Redistribution subject to ASA license or copyright; see http://acousticalsociety.org/content/terms. Download to IP: 132.177.229.80 On: Tue, 17 Nov 2015 15:33:38

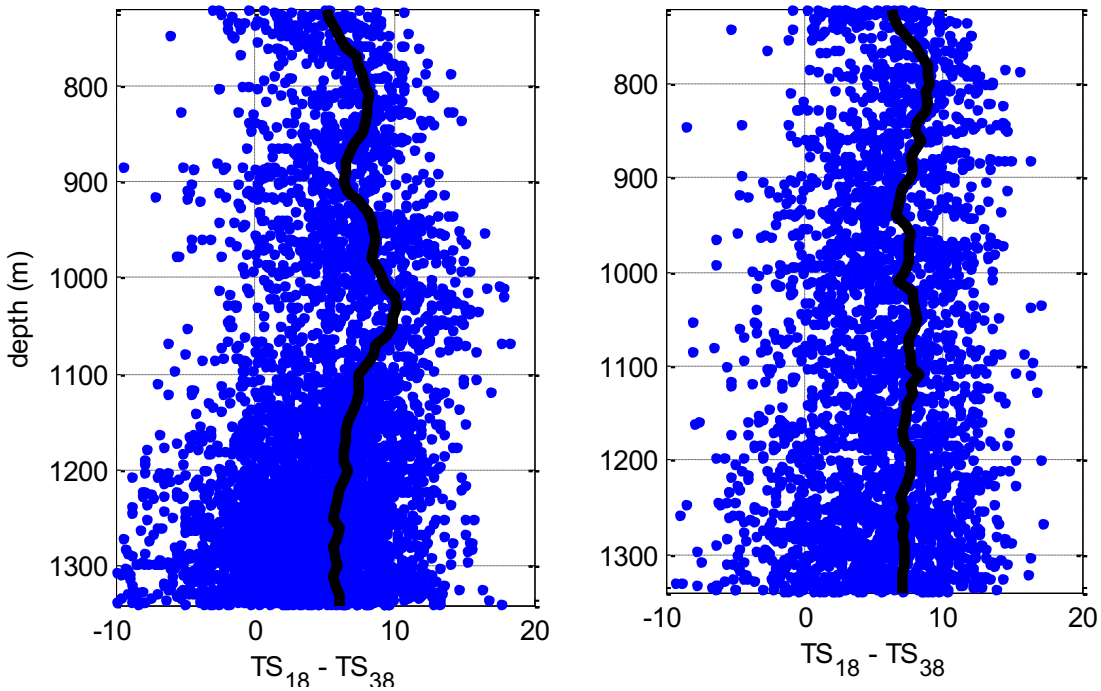

Figure 4. Target strength difference (TS_{18}-TS_{38}) for seeps 1 (left) and 2 (right) shown in Figure 1.

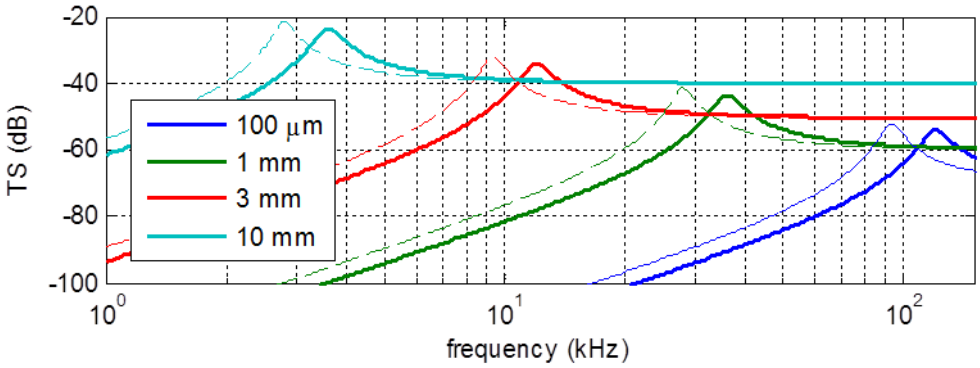

Figure 5. Target strength for individual bubbles of radius 0.1, 1, 5, and 10 mm at water depths of 1340 m (solid line) and 800 m (dashed line).

5 CONCLUSIONS

Methane seeps that are manifested as gas bubbles in the water column are strong acoustic targets that are often detectable with split-beam echosounders mounted on surface vessels. In addition to detecting the presence or absence of the gas seeps, split-beam echosounders can be used to assess the seep morphology (e.g., height and vertical trajectory) and if multiple frequencies are available, the frequency difference information can be used to constrain the nominal bubble size as a function of depth. Together, these data provide evidence of the complicated evolution of deep-ocean methane bubbles as they rise through the water column, acquiring a hydrate coating in the deep water and

Redistribution subject to ASA license or copyright; see http://acousticalsociety.org/content/terms. Download to IP: 132.177.229.80 On: Tue, 17 Nov 2015 15:33:38

eventually out-gassing into the surrounding seawater unless some other mechanism (e.g., oil coatings [5]) substantially slows the gas transfer above the hydrate dissociation depth. In addition to providing information describing the complicated evolution of the gas bubbles, the bubble trajectories also provide information on deep ocean currents.

ACKNOWLEDGEMENTS

This work was supported under NOAA grant NA05NOS4001153. We would like to acknowledge the captain and crew of the *Gordon Gunter* for their assistance during the collection of this data.

REFERENCES

1. Weber, T., A. De Robertis, S. Greenaway, S. Smith, L. Mayer, and G. Rice, Estimating oil concentration and flow rate with vessel-mounted acoustic echo sounders, *Proc. Nat. Acad. Sci.*, doi:10.1073/pnas.1108771108. (2011).
2. Roberts, H.H. and R.S. Carney, Evidence of episodic fluid, gas, and sediment venting on the northern Gulf of Mexico continental slope. *Economic Geology* 92:863-879. (1997).
3. Judd, A.G., Natural seabed gas seeps as sources of atmospheric methane, *Environmental Geology* 46, 099-996. (2004)
4. Fisher, C., H. Robers, E. Cordes, and B. Bernard Cold seeps and associated communities of the Gulf of Mexico, *Oceanography* 20(4). (2007)
5. MacDonald, I. R., I. L. R. Sassen, P. Stine, R. Mitchell, and N. J. Guinasso Transfer of hydrocarbons from natural seeps to the water column and atmosphere, *Geofluids*, 2, 95–107. (2002)
6. Rehder, G., P. Brewer, E. Peltzer, and G. Friedrich, Enhanced lifetime of methane bubble streams within the deep ocean, *Geophysical Research Letters,* 29(15). (2002).
7. Merewether, R., M.S. Olsson, P. Lonsdale, Acoustically detected hydrocarbon plumes rising from 2-km depths in the Guayamas Basin, Gulf of California, *J. Geophys. Res*. 90, 3075-3085 (1985).
8. Dimitrov, L., V. Dontcheva, Seabed pockmarks in the southern Bulgarian Black Sea zone, *Bull. Geol. Soc. Den*. 41, 24-33. (1994).
9. Hornafius, J., D. Quigley, B. Luyendyk, The world's most spectactular marine hydrocarbon seeps (Coal Oil Point, Santa Barbar Channel, California): quantification of emission*, J. Geophys. Res.* 104, 20703-20711. (1999).
10. Heeschen, K., A. Trehu, R. Collier, E. Suess, and G. Rehder, Distribution and height of methane bubble plumes on the Cascadia Margin characterized by acoustic imaging, *Geophys. Res. Let* 30. (2003).
11. Greinert, J., Y. Artemov, V. Egorov, M. De Batist, and D. McGinnis, 1300-m-high rising bubbles from mud volcanos at 2080 m in the Black Sea: Hydroacoustic characteristics and temporal variability, *Earth and Plan. Sci. Let*. 244. (2006).
12. Burdic, W., *Underwater Acoustic System Analysis.* Englewood Cliffs, NJ: Prentice Hall. (1984)
13. Lurton, X., Swath bathymetry using phase difference: theoretical analysis of acoustical measurement precision, *IEEE J. Oce. Eng*. 25(3). (2000)
14. McGinnis, D., J. Greinert, Y. Artemov, S. Beaubien, and A. Wuest, Fate of rising methane bubbles in stratified waters: How much methane reaches the atmosphere?, *J. Geophys. Res*. 111. (2006).
15. Tishchenko, P., C. Hensen, K. Wallmann, C. Wong, Calculation of the stability and solubility of methane hydrate in seawater, *Chem. Geo.* 219, 37-52. (2005).
16. Foote, K., H. Knudsen, G. Vestnes, D. MacLennan, and J. Simmonds, Calibration of acoustic instruments for fish density estimation: a practical guide. *ICES Cooperative Research Report, 144*. 69 pp. (1987)

Redistribution subject to ASA license or copyright; see http://acousticalsociety.org/content/terms. Download to IP: 132.177.229.80 On: Tue, 17 Nov 2015 15:33:38